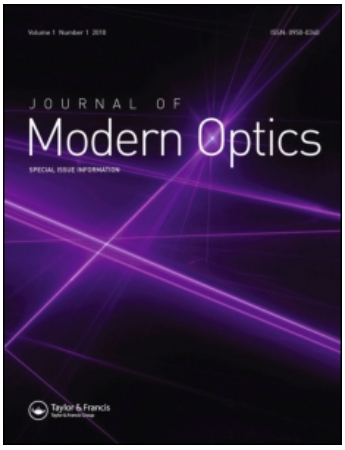

Journal of Modern Optics
Publication details, including instructions for authors and subscription information:
http://www.informaworld.com/smpp/title~content=t713191304

Fibre-coupled, single photon detector based on NbN superconducting nanostructures for quantum communications

W. Słysz[ab]; M. Wegrzecki[a]; J. Bar[a]; P. Grabiec[a]; M. Górska[a]; V. Zwiller[cd]; C. Latta[c]; P. Böhi[c]; A. J. Pearlman[b]; A. S. Cross[b]; D. Pan[b]; J. Kitaygorsky[b]; I. Komissarov[b]; A. Verevkin[be]; I. Milostnaya[f]; A. Korneev[f]; O. Minayeva[f]; G. Chulkova[f]; K. Smirnov[f]; B. Voronov[f]; G. N. Gol'tsman[f]; Roman Sobolewski[b]
[a] Institute of Electron Technology, 02-668 Warsaw, Poland [b] Department of Electrical and Computer Engineering and Laboratory for Laser Energetics, University of Rochester, Rochester, NY 14627-0231, USA [c] Quantum Photonics, Swiss Federal Institute of Technology, Zurich, 8093 Zurich, Switzerland [d] Kavli Institute of Nanoscience Delft, Delft University of Technology, 2600 GA Delft, The Netherlands [e] Department of Electrical Engineering, SUNY University at Buffalo, Buffalo, NY 14260, USA [f] Department of Physics, Moscow State Pedagogical University, Moscow 119435, Russia

To cite this Article Słysz, W. , Wegrzecki, M. , Bar, J. , Grabiec, P. , Górska, M. , Zwiller, V. , Latta, C. , Böhi, P. , Pearlman, A. J. , Cross, A. S. , Pan, D. , Kitaygorsky, J. , Komissarov, I. , Verevkin, A. , Milostnaya, I. , Korneev, A. , Minayeva, O. , Chulkova, G. , Smirnov, K. , Voronov, B. , Gol'tsman, G. N. and Sobolewski, Roman(2007) 'Fibre-coupled, single photon detector based on NbN superconducting nanostructures for quantum communications', Journal of Modern Optics, 54: 2, 315 — 326
To link to this Article: DOI: 10.1080/09500340600779496
URL: http://dx.doi.org/10.1080/09500340600779496

Journal of Modern Optics
Vol. 54, Nos. 2–3, 20 January–15 February 2007, 315–326

Fibre-coupled, single photon detector based on NbN superconducting nanostructures for quantum communications

W. SŁYSZ†‡, M. WĘGRZECKI†, J. BAR†, P. GRABIEC†, M. GÓRSKA†, V. ZWILLER§¶, C. LATTA§, P. BÖHI§, A. J. PEARLMAN‡, A. S. CROSS‡, D. PAN‡, J. KITAYGORSKY‡, I. KOMISSAROV‡, A. VEREVKIN‡‖, I. MILOSTNAYA‖‖, A. KORNEEV‖‖, O. MINAYEVA‖‖, G. CHULKOVA‖‖, K. SMIRNOV‖‖, B. VORONOV‖‖, G. N. GOL'TSMAN‖‖ and ROMAN SOBOLEWSKI*‡

†Institute of Electron Technology, Al. Lotników 32/46, 02-668 Warsaw, Poland
‡Department of Electrical and Computer Engineering and Laboratory for Laser Energetics, University of Rochester, Rochester, NY 14627-0231, USA
§Quantum Photonics, Swiss Federal Institute of Technology, Zurich, 8093 Zurich, Switzerland
¶Kavli Institute of Nanoscience Delft, Delft University of Technology, 2600 GA Delft, The Netherlands
‖Department of Electrical Engineering, SUNY University at Buffalo, Buffalo, NY 14260, USA
‖‖Department of Physics, Moscow State Pedagogical University, Moscow 119435, Russia

(*Received 28 February 2006; in final form 24 April 2006*)

We present a novel, two-channel, single photon receiver based on two fibre-coupled, NbN, superconducting, single photon detectors (SSPDs). The SSPDs are nanostructured superconducting meanders and are known for ultrafast and efficient detection of visible-to-infrared photons. Coupling between the NbN detector and optical fibre was achieved using a micromechanical photoresist ring placed directly over the SSPD, holding the fibre in place. With this arrangement, we obtained coupling efficiencies up to ~30%. Our experimental results showed that the best receiver had a near-infrared system quantum efficiency of 0.33% at 4.2 K. The quantum efficiency increased exponentially with the photon energy increase, reaching a few percent level for visible-light photons. The photoresponse pulses of our devices were limited by the meander high kinetic inductance and had the rise and fall times of approximately 250 ps and 5 ns, respectively. The receiver's timing jitter was in the 37 to 58 ps range, approximately 2 to 3 times larger than in our older free-space-coupled SSPDs. We stipulate that this timing jitter is in part due to optical fibre properties. Besides quantum communications, the two-detector arrangement should also find applications in quantum correlation experiments.

*Corresponding author. Email: roman.sobolewski@rochester.edu

Journal of Modern Optics
ISSN 0950–0340 print/ISSN 1362–3044 online © 2007 Taylor & Francis
http://www.tandf.co.uk/journals
DOI: 10.1080/09500340600779496

1. Introduction

Modern quantum communications (QC) is currently an area of science that is under intense investigation. QC provides a unique possibility of ultrafast, extremely low power and unconditionally secure information exchange. Optical QC systems require photon counters with high speed, high sensitivity, high quantum efficiency (QE), and short dead times along with precise timing characteristics and low dark counts [1]. For QC systems with optical fibres, detectors working at standard near-infrared (NIR) telecommunication wavelengths of 1.3 μm and/or 1.55 μm are needed.

The most popular single photon detectors (SPDs), semiconductor avalanche photodiodes (APDs), have a limited utility for QC applications [2]. Si APDs have their sensitivity restricted by the Si bandgap (1.1 μm); therefore, they cannot be directly implemented in fibre optic communication networks. The InGaAs APDs work in the NIR region and the best devices (in the 1.2 to 1.6 μm wavelength range) have a QE of >20% in single photon detection mode, but their timing jitter is 50 ps or longer and they suffer from very high (>10 kHz) dark counts [3, 4]. All APDs have to be gated and either passively or actively quenched to reduce the dark-count noise.

Another very promising SPD that was recently developed is a transition-edge sensor (TES) [5]. The TES is a superconducting tungsten bolometer and, because of its extreme high sensitivity, it exhibits photon number resolving capabilities and QE >86% [6]. It operates at temperatures $T < 100$ mK and has almost negligible dark counts [7]. These devices, however, suffer greatly from a 4 μs recovery time and a 72 ns full width at half maximum (FWHM) arrival time resolution (jitter). Nevertheless, TESs have been successfully implemented in a QC channel, although operating at a low counting rate [7].

Another type (besides TES) of a superconducting SPD (SSPD) recently developed is an ultra-thin, submicron-width NbN structure maintained at T far below the NbN critical temperature T_c [8, 9]. The SSPD operation principle has been explained within a phenomenological hot-electron photoresponse model [10, 11]. As we have already presented, the NbN SSPDs are ultrafast and efficiently count photons with wavelengths ranging from ultraviolet to infrared. They have already been successfully used for free-space (laboratory) detection at fibre communication wavelengths [9].

We present here a double-channel, fibre-coupled receiver designed for telecommunication wavelengths and prepared for simultaneous detection of two polarizations of single photons in practical QC systems as well as for antibunching-type quantum correlation studies. The receiver is based on two fibre-coupled NbN SSPDs operating at 4.2 K inside a liquid-helium dewar. Both the fibre and electrical connections, however, are outside the dewar at room temperature.

2. Construction of the receiver

The NbN SSPDs were fabricated according to a technological procedure described in detail in [12]. Most of the detectors used in our receiver were $10 \times 10\,\mu m^2$ superconducting meander-type structures with a 4 nm thickness and a 120 nm

nominal strip width. Recently, we also used $10 \times 20\,\mu m^2$ devices. The critical current density J_c of the completed devices varied within 2 to $6\,MA\,cm^{-2}$ at 4.2 K with $T_c \sim 10\,K$. The general idea of the receiver construction is presented in figure 1. The receiver was designed to be immersed and operated in a standard liquid helium transport dewar.

The system consists of two independent detector channels (figure 1). In each channel, the photon delivery to the NbN detector is provided by the single/multi-mode fibre, while the electrical output is connected to the room-temperature electronics via a SMA connector directly integrated with the SSPDs coplanar waveguide output. A picture of the receiver's bottom flange with both the fibre and electrical connections is shown in figure 1(*a*). Figure 1(*b*) presents a cross-section through the fibre coupling mechanical support, which consists of a micromechanical photoresist ring and two bridge-like aluminium holders.

The photoresist ring is positioned over the SSPD meander structure with an accuracy of 1 μm using a photolithography process guided by alignment marks made on the SSPD during its fabrication process [13]. The fibre, stripped of its jacket, is pushed against the NbN film and permanently attached with optical glue.

As indicated in figure 1, each electrical trace is connected through a bias-tee to an electronics box containing a biasing circuit and a two-stage, broadband amplifier with a 62 dB total gain and 0.05 to 4 GHz bandwidth. The bias-tee and the electronics box operate outside the dewar, and the optical fibre is connected directly to the source of photons using a standard FC connector. Mechanical details of the entire apparatus and the methods of joining them together were optimized with

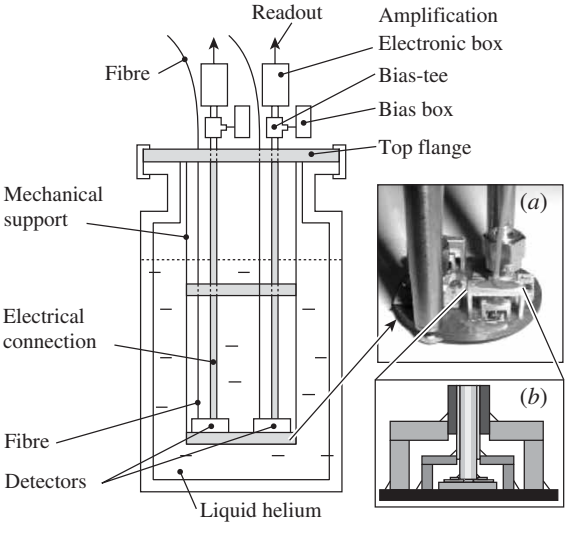

Figure 1. Schematic of a two-channel single photon detector operating in a helium transport dewar. (*a*) Detail of a cryogenic end, SMA connectors and detectors pigtailed to fibres. (*b*) Cross-section of the fibre-coupling scheme.

respect to mechanical stability and resistance to thermal stress associated with room temperature-to-helium cycling.

During the experiments, the receiver was placed in a standard (60 l) liquid-He transport dewar. One container was sufficient for over two months of permanent operation. During this period, for robustness test purposes, the receiver was taken out of the dewar many times (on average 1–2 times per week) and immersed again with no observed deterioration in its performance and no visible or measurable mechanical damage. Only the initial (first) cooling of the detector insert sometimes resulted in the catastrophic failure of our apparatus, which was later traced to fibre microcracking.

3. Experimental results

3.1 *System quantum efficiency*

We fabricated ten efficient receivers (five pairs), eight of which were coupled via single-mode fibres and two utilized multimode fibres. The main figure of merit was the system QE (SQE) for each receiver [9, 14, 15]. We used highly attenuated, 41 ps wide pulses from a semiconductor laser diode operating at a 1540 nm wavelength with a repetition rate of 1 MHz. The optical power delivered to the detectors was controlled with a calibrated, digital optical attenuator. We measured the nominal optical power at the room temperature end of the fibre (at the FC connector plane) and the subsequent relative levels were obtained using the attenuator. Next, the optical power values were divided by the photon ($\lambda = 1540$ nm) energy to calculate the photon flux, which, in turn, was divided by the laser repetition rate (1 MHz) to obtain the average number of photons per optical pulse.

The output signals from the amplifiers (located inside the electronics boxes) were connected to either a fast oscilloscope for time-resolved studies or to a signal counter to perform statistical analysis of our photon counts or to measure the dark counts.

The typical dependences of the detection probability (DP) versus the number of photons per optical pulse incident on the NbN detector for a number of our receivers are presented in figure 2. At high power levels, we observe a saturation of DP at a value close to 100%, as the receiver is able to count all laser pulses. At low-incident photon fluxes, our experimental data show a linear dependence of DP versus the number of incident photons over five orders of magnitude, demonstrating the single photon detection mechanism [6]. The behaviour observed in figure 2 agrees well with our previous observations [3, 6]. Taking the DP value measured for $I_b \approx 0.95 I_c$ at the photon flux level corresponding to an average of one photon per pulse; we determined the SQE of our receivers and listed the values for the best and weakest devices directly above figure 2 and in table 1. We also present in this table the corresponding device QE (DQE) values characteristic to the detector structure and measured directly after the SSPD fabrication. Finally, table 1 contains the ratio SQE/DQE, which is an experimental measure of the efficiency of

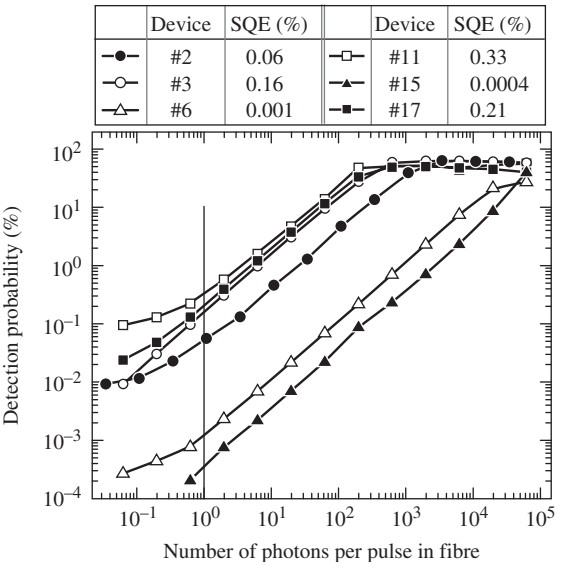

Figure 2. Photoresponse detection probability versus the averaged number of photons per pulse for several fibre-coupled NbN SSPDs illuminated by 1540 nm wavelength photons. The thin vertical line indicates the 1 photon/pulse flux and corresponds to the SQE definition.

Table 1. DQE, SQE and calculated K values for fibre-coupled SSPD receivers operating at the telecommunication 1.55 μm wavelength.

Detector number number	DQE (%)	SQE (%)	K	Fibre	
2	2.1	0.06	0.029	Single mode	
3	4.9	0.16	0.033	Multimode	Best
11	1.0	0.33	0.333	Single mode	receivers
17	6.4	0.21	0.033	Single mode	
6	2.0	0.001	0.0005	Single mode	Weak
15	2.1	0.0004	0.0002	Single mode	receivers

fibre coupling K. We note that device #11 exhibits the best SQE = 0.33% and $K = 0.33$.

The separate dark-count measurements with the fibre input blocked (0 photons per pulse) resulted in 2 (device #6) to 90 (device #11) counts per second for a bias current $I_b \approx 0.95 I_c$. Such low dark counts allowed us to measure 'live' photon counts at fluxes as low as 0.06 photons per pulse. At this level, our signal-to-background ratio was roughly 2. We note that the dark-count rates measured in fibre-coupled SSPDs are somewhat larger than in our earlier free-space devices [9]. We tentatively associate these excess dark counts with the 300 K background radiation picked by the fibre's room temperature end.

To analyse the fibre-coupling performance, we computed K between the detector and fibre, assuming a perfect Gaussian mode-light profile emitted from the fibre. We obtain the fraction K of power incident on the square ($10 \times 10\,\mu m^2$) detector with side length a

$$K = \frac{2}{\pi w_0^2\left[1 + \left(\lambda z/\pi w_0^2\right)^2\right]} \int_{-a/2}^{a/2} \int_{-a/2}^{a/2} \exp\left\{\frac{-2\left(x^2 + y^2\right)}{w_0^2\left[1 + \left(\lambda z/\pi w_0^2\right)^2\right]}\right\} \mathrm{d}x\,\mathrm{d}y, \qquad (1)$$

where w_0 is the beam radius and λ is the optical wavelength.

In our calculations, we did not take into account the detectors' reflection or transparency because we wanted to determine the expected SQE values for our receiver, knowing the DQE value, and compare them to those listed in table 1.

The resulting calculations, based on equation (1) for the detector–fibre misalignment, are presented in figure 3, which shows the constant K values for the increasing vertical fibre–SSPD distance (y axis) and the horizontal (radial) fibre misalignment (x axis). We see that there is a rather weak dependence of K on the vertical fibre–detector separation. For perfect horizontal alignment and the most probable detector-to-fibre distance of 5 to 10 μm, we expect to have Ks as large as 0.9.

As seen in figure 3, the horizontal plane misalignment is the most significant determinant in the diminishing value of K. Since at room temperature the fibre was precisely positioned with the photoresist ring, the misalignment and the resulting low K observed in our devices (see table 1 and figure 3) were most likely due to the distortion (tilt) of the fibre end face with respect to the SSPD plane that was caused by its uncontrolled cryogenic contraction and horizontal movement during the cooldown process. Therefore, the 30 μm-thick positioning ring appears to be

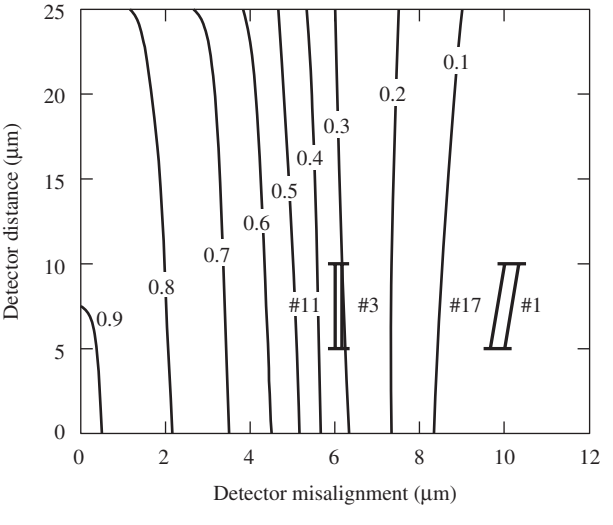

Figure 3. Dependence of the coupling factor K versus the detector–fibre misalignment distance. The measured values of K for four detectors from table 1 are placed on the diagram.

insufficiently resistant to lateral distortions of the fibre, resulting in lower than expected *K*s, experimentally observed in most of our devices (see table 1).

In an attempt to improve the fibre alignment and reduce the lateral distortions, we implemented a multimode fibre in our detectors. Because of the large ~50 μm diameter core of the multimode fibre, the coupling should be less sensitive to fibre displacement in the *x*–*y* plane. Unfortunately, the *K* value listed in table 1 (see also figure 2) for the multimode fibre-coupled detector does not support the above expectations. One should note, however, that in the case of the multimode fibre, because of the large (~2000 μm^2) core area, only a small portion of radiation reaches the detector with a much smaller (100 μm^2) surface area. Assuming a Gaussian power distribution in the graded-index core, we can estimate that only 1/10 of the power from the fibre reaches the SSPD, even in the case of perfect horizontal alignment. Moreover, it is well known that multimode fibres suffer from a speckle noise. Since the size of the detector is much less than the size of the fibre core, it is very likely that our QE measurement was affected by the speckle noise.

Table 1 also shows that some of our detectors exhibited very low SQE and *K* values. In these cases, the most probable reason was either a cooling-related crack of the fibre somewhere along its length or a permanent deformation/contraction of the fibre's ending position with respect to the NbN meander. Evidence of this is that *K* remained constant after a few thermal cycles, and cracks in the fibres were found in mechanical post-mortem tests of the two weakest devices.

The QE values presented in table 1 are significantly lower than those for the SSPDs reported in our previous publications. We need to stress, however, that in our receiver, the SQE value is not merely the efficiency of the detector, but also includes that of the fibre-coupling arrangement.

Figure 4 shows the spectral dependence of the SQEs for two fibre-coupled receivers. We note that both data sets follow exponential dependences with the same slope, meaning that the SSPD photoresponse mechanism is the same as reported earlier by us and is based on the hot-spot formation and current redistribution model [10, 11]. Thus, the differences in the actual SQE values for a given receiver can be accounted by the spectral dependence of DQE, however, we cannot exclude that *K* also depends on the incident photon wavelength.

3.2 *Timing parameters*

As demonstrated by Kerman *et al.* [16], for large meander-type SSPDs, the photoresponse pulse width and its fall time are limited by the large kinetic inductance of the superconducting meander. For our time-resolved measurements, we used the experimental set-up that consisted of a bias-tee (80 kHz to 26 GHz) semiconductor laser ($\lambda = 1.55\,\mu m$), a broadband amplifier (50 MHz to 4 GHz) and a 6 GHz, Tektronix, single-shot digital oscilloscope. An example of the photoresponse transient of our fibre-coupled detector is shown in figure 5 (dotted line) and consists a ~250 ps rise time and a ~5 ns fall time, with a FWHM of about 2.5 ns. This figure also presents a typical dark-count pulse (light solid line) observed with the fibre input completely blocked. We note that the shape of the dark-count pulse is

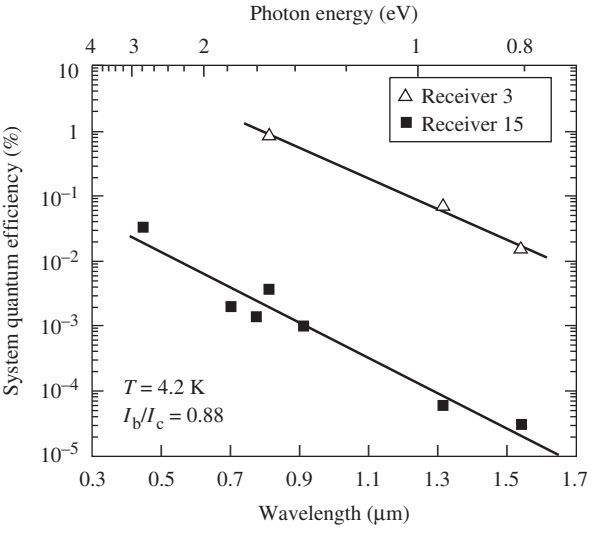

Figure 4. Spectral dependences of the SQE for the multimode receiver #3 and single-mode receiver #15. In order to directly compare the SQE values for two different devices in a wide photon-energy (wavelength) range, all the data points were obtained for the bias current $I_b = 0.88I_c$. Thus, the SQE values shown in the figure for 1540 nm photons are somewhat lower than those listed in table 1.

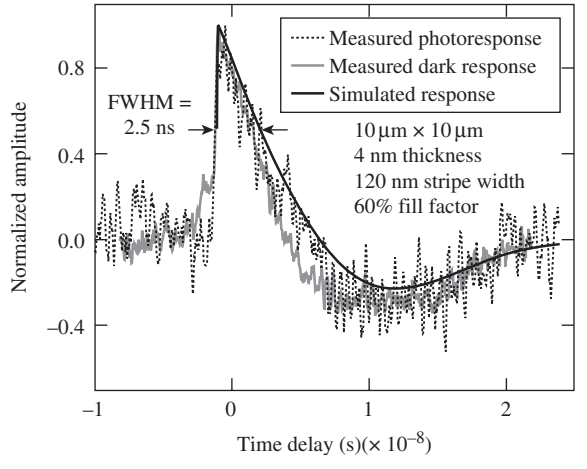

Figure 5. Measured photoresponse signal (dotted line) and dark response (light solid line) of our fibre-coupled NbN detector compared with theoretical calculation (dark solid line), based on the kinetic inductance model [16].

identical with the photoresponse pulse, indicating that in both cases the output signal is limited by the extrinsic kinetic inductance.

The latter conclusion was directly confirmed by our theoretical calculations of the pulse shape, taking into account the true dimensions of the NbN SSPD: thickness

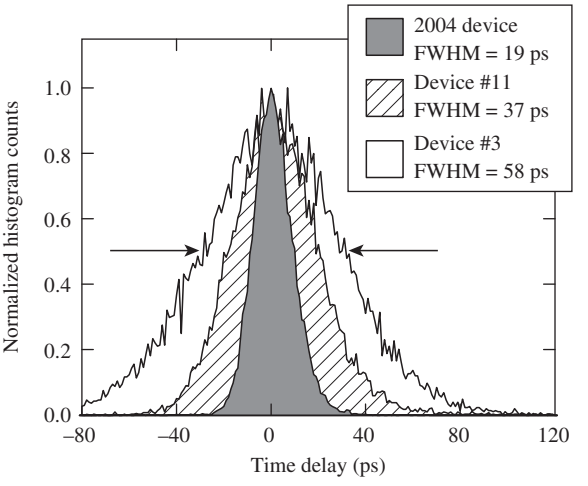

Figure 6. Jitter comparison of NbN free-space and fibre-coupled SSPDs at a 1540 nm wavelength. Free-space device reported in [9] with a jitter of 19 ps FWHM. Single-mode fibre-coupled device with a jitter of 37 ps FWHM. Multimode fibre-coupled device with a jitter of 58 ps FWHM.

$d = 4$ nm, stripe width $w = 120$ nm, and an 80 nm gap between the stripes. Using these dimensions, we calculated the kinetic inductance, using the FastHenry inductance simulation program, version 3.0 [17] and assuming a London penetration depth of $\lambda_L = 560$ nm, as estimated by Hadfield *et al.* [18]. We have also verified that when we used this penetration depth value to calculate inductances of our devices, they matched the measured values for the devices used in [16]. The actual calculated inductance value was 420 nH, in good agreement with a simple expression for the kinetic inductance of a thin superconducting film of length l with $d, w \ll \lambda_L$;

$$L_k = \mu_0 \lambda_L^2 \frac{l}{wd}. \tag{2}$$

Following the inductance model used by Kerman *et al.* [16], we then simulated the voltage response and filtered the signal according to our experimental set-up bandwidth, measured with a spectrum analyser. The theoretical fit (dark solid line in figure 5) overlaps almost perfectly with our experimental data, confirming that indeed in large-area, meander-type SSPDs, the output signal is limited by the device extrinsic kinetic inductance.

In the same experimental setup as above, we also measured the timing jitter of our fibre coupled detectors. The experimental data are shown in figure 6 and were collected using the standard histogram feature installed in a 50 GHz Tektronix sampling oscilloscope. For comparison, we also included the timing fitting of one of our older, free-space-coupled SSPDs [9]. We note that the jitter profile in all cases is Gaussian and for fibre-coupled structures the FWHM varies from 37 ps for a

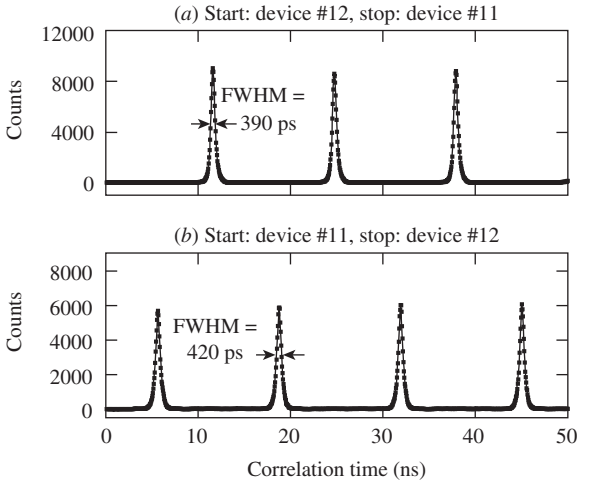

Figure 7. Correlation measurements on 82 MHz laser pulses, performed with a two-channel, fibre-coupled SSPD receiver. (*a*) High-SQE device #11 as a stop detector. (*b*) Low-SQE device #12 as a stop detector.

single-mode detector to ~60 ps for the multimode one. In both cases, the timing jitter is higher than that for the free-space SSPD, apparently, because of the ~2 m long fibres and electrical output cables implemented in our cryogenic insert (figure 1). In addition, in multimode fibres, we need to take into account a speckle noise and substantial modal dispersion.

To further test the timing resolution of our complete detector systems and determine their usefulness for applications in photon quantum-correlation experiments, we carried out our own correlation experiments with two SSPD detectors placed on one flange of our receiver. The pulsed laser light was split by a 50/50 beam splitter and detected by the two detectors. The signal from each detector was sent to a discriminator and fed to a correlator. In figure 7(*a*), detector #12 with a low SQE (~0.005%) operated as a start device and the high SQE detector #11 acted as a stop. We used 500 fs wide pulses at $\lambda = 940$ nm with a repetition rate of 82 MHz. The correlation time (FWHM of 390 ps), presented in figure 7(*a*), can be regarded as the time resolution of the complete correlation system (amplifiers, discriminator, correlator, cables, terminators and detectors).

Figure 7(*b*) shows the correlation measurements with the start and stop detectors reversed. As expected, the correlation width (430 ps FWHM) is virtually identical and only the total number of collected counts decreases. The widths of the correlation traces shown in figure 7 are relatively narrow compared to standard APD quantum correlation systems, but wider compared to a combination APD–SSPD system presented in [19]. The latter results demonstrate the utility of SSPDs in general and our fibre-coupled devices in particular for quantum-correlation-type measurements [20].

4. Conclusions

We have fabricated and tested a number of fibre-based, single photon receivers designed for applications in optical QC systems. The SQE of our best detector in NIR was measured as 0.33%; however, we expect to reach values as high as 3% to 5%. This will be accomplished by implementing SSPDs with higher DQE values since the estimated coupling efficiency of the fibre–detector set-up in our design has already reached 30%. Microlenses and thicker (e.g. 50 μm thick) photoresist rings should increase that coupling efficiency even further.

Our fully integrated two-channel, single photon detectors were placed inside the sealed helium transport dewar with SSPDs maintained at $T = 4.2\,\mathrm{K}$, while the optical and electrical connections remained at room temperature. The system operating time between helium refills was above 2 months. Therefore, from an external operator's point of view, our whole receiver could be regarded as a 'room-temperature-like' apparatus. The performance parameters, such as $>200\,\mathrm{MHz}$ photon-counting rate, $<40\,\mathrm{ps}$ timing jitter, and $<100\,\mathrm{Hz}$ dark counts, make our SSPD receivers especially useful for such applications as practical quantum key distribution, in which photons with two separate polarizations (e.g. vertical and horizontal) can be simultaneously counted using two parallel channels. The other forthcoming application is in the photon quantum-correlation measurements.

Acknowledgements

The authors would like to thank Dr Marc Currie for his assistance in time-resolved photoresponse measurements and Professor Atac Imamoglu for his support. This work was supported by the Polish Ministry of Science under Project No. 3 T11B 052 26 (Warsaw); RFBR 03-02-17697 and INTAS 03-51-4145 (Moscow); CRDF grants RE2-2531-MO-03 (Moscow) and RE2-2529-M0-03 (Moscow and Rochester); and AFOSR grant FA9560-04-1-0123 (Rochester). Additional financial support was provided by the MIT Lincoln Laboratory and BBN Technologies.

References

[1] J.C. Livas, E.A. Swanson, S.R. Chinn, *et al.*, in *Free-Space Laser Communication Technologies VII*, Vol. 2381, edited by G.S. Mecherle (SPIE, Bellingham, WA, 1995), p. 38.
[2] C. Kurtsiefer, P. Zarda, M. Halder, *et al.*, in *Quantum Optics in Computing and Communications*, Vol. 4917, edited by S. Liu, G. Guo, H.-K. Lo and N. Imoto (SPIE, Bellingham, WA, 2002), p. 25.
[3] Y. Kang, Y.-H. Lo, M. Bitter, *et al.*, Appl. Phys. Lett. **85** 1668 (2004).
[4] G. Ribordy, N. Gisin, O. Guinnard, *et al.*, J. Mod. Opt. **51** 1381 (2004).
[5] B. Cabrera, R.M. Clarke, P. Colling, *et al.*, Appl. Phys. Lett. **73** 735 (1998).
[6] D. Rosenberg, A.E. Lita, A.J. Miller, *et al.*, Phys. Rev. A **71** 061803(R) (2005).
[7] D. Rosenberg, S.W. Nam, P.A. Hiskett, *et al.*, Appl. Phys. Lett. **88** 021108 (2006).
[8] A. Verevkin, A. Pearlman, W. Słysz, *et al.*, J. Mod. Opt. **51** 1447 (2004).
[9] A. Korneev, P. Kouminov, V. Matvienko, *et al.*, Appl. Phys. Lett. **84** 5338 (2004).

[10] G.N. Gol'tsman, O. Okunev, G. Chulkova, *et al.*, Appl. Phys. Lett. **79** 705 (2001).
[11] A.D. Semenov, G.N. Gol'tsman and A.A. Korneev, Physica C **351** 349 (2001).
[12] G.N. Gol'tsman, K. Smirnov, P. Kouminov, *et al.*, IEEE Trans. Appl. Supercond. **13** 192 (2003).
[13] P. Grabiec, W. Słysz, M. Węgrzecki, *et al.*, Poland Patent No. P-367391 (patent pending, 2004).
[14] A. Verevkin, J. Zhang, R. Sobolewski, *et al.*, Appl. Phys. Lett. **80** 4687 (2002).
[15] W. Słysz, M. Węgrzecki, J. Bar, *et al.*, in *Infrared Photoelectronics*, Vol. 5957, edited by A. Rogalski, E.L. Dereniak and F.F. Sizov (SPIE, Bellingham, WA, 2005), p. 310.
[16] A.J. Kerman, E.A. Dauler, W. Keicher, *et al.*, Appl. Phys. Lett. **88** 111116 (2006).
[17] Software available at http://www.wrcad.com/freestuff.html, Whiteley Research Inc., Sunnyvale, CA, 94086.
[18] R.H. Hadfield, A.J. Miller, S.W. Nam, *et al.*, Appl. Phys. Lett. **87** 203505 (2005).
[19] R.H. Hadfield, M.J. Stevens, S.S. Gruber, *et al.*, Opt. Express **13** 10846 (2005).
[20] Z.Y. Ou and L. Mandel, Phys. Rev. Lett. **61** 50 (1988).